Journal of Intelligent & Fuzzy Systems 45 (2023) 1757–1774
DOI:10.3233/JIFS-223897
IOS Press

Fuzzy-Rough induced spectral ensemble clustering

Guanli Yue[a], Ansheng Deng[a,*], Yanpeng Qu[b], Hui Cui[a] and Jiahui Liu[a]
[a]*Information Science and Technology College, Dalian Maritime University, Dalian, China*
[b]*School of Artificial Intelligence, Dalian Maritime University, Dalian, China*

Abstract. Ensemble clustering helps achieve fast clustering under abundant computing resources by constructing multiple base clusterings. Compared with the standard single clustering algorithm, ensemble clustering integrates the advantages of multiple clustering algorithms and has stronger robustness and applicability. Nevertheless, most ensemble clustering algorithms treat each base clustering result equally and ignore the difference of clusters. If a cluster in a base clustering is reliable/unreliable, it should play a critical/uncritical role in the ensemble process. Fuzzy-rough sets offer a high degree of flexibility in enabling the vagueness and imprecision present in real-valued data. In this paper, a novel fuzzy-rough induced spectral ensemble approach is proposed to improve the performance of clustering. Specifically, the significance of clusters is differentiated, and the unacceptable degree and reliability of clusters formed in base clustering are induced based on fuzzy-rough lower approximation. Based on defined cluster reliability, a new co-association matrix is generated to enhance the effect of diverse base clusterings. Finally, a novel consensus spectral function is defined by the constructed adjacency matrix, which can lead to significantly better results. Experimental results confirm that the proposed approach works effectively and outperforms many state-of-the-art ensemble clustering algorithms and base clustering, which illustrates the superiority of the novel algorithm.

Keywords: Rough set, fuzzy-rough set, ensemble clustering, cluster reliability, spectral clustering

1. Introduction

Clustering is an unsupervised learning method that usually refers to dividing existing unlabeled instances into several clusters according to the similarity between objects without any prior information, making the instances in the same cluster have a higher similarity and in different clusters have a more substantial discrepancy [9, 11, 43]. Ensemble clustering utilises a consensus function to unify multiple types of partitions of the same dataset into one clustering result. It usually constructs a base clustering pool by repeatedly running a single clustering approach or executing multiple clustering algorithms. Then, the consensus function is built through voting methods, hypergraph partitioning, or evidence accumulation to obtain more optimal clustering results [18, 25]. Many existing ensemble clustering studies have confirmed that ensemble clustering can usually improve the clustering result compared to a single clustering algorithm [1, 14, 24].

1.1. Background

Existing established clustering algorithms are mainly based on the theories of model, grid, density, partition, and hierarchy [2, 8]. Different types of clustering algorithms are good at solving diverse types, distributions, and scales of data. In particular, with the development of deep learning [27], the performance of various clustering methods has been further

*Corresponding author. Ansheng Deng, Information Science and Technology College, Dalian Maritime University, Dalian, China. E-mail: ashdeng@dlmu.edu.cn.

improved. For example, in [28], a deep-learning feature extractor for time-series data is designed for relation extraction, and the clustering effect achieved significant improvement. Nonetheless, in view of the unknown data distribution in actual problems, it is difficult to determine which clustering algorithm can get better clustering results. Conventional solutions often try different methods and choose the algorithm that performs best. Ensemble clustering is expected to establish a general scheme to combine the advantages of multiple clustering algorithms and form the optimal clustering result. It is especially feasible under the conditions of mature distributed computing technology, so as to adapt to unknown and complex data.

The related studies to ensemble clustering are mainly divided into three categories: pair-wise co-occurrence based, graph partitioning based, and median partition based algorithms [18]. The first type refers to constructing a co-occurrence matrix by finding the times of all instances that occur in pairs (assigned as a cluster) in base clusterings. The two instances should be classified into the same cluster in the final clustering based on co-occurrence [19]. The similarity function constructed by the co-occurrence matrix can be used in any similarity matrix based clustering algorithm to acquire the final optimal clustering result, such as hierarchical clustering and spectral clustering [7, 30]. The idea of co-occurrence matrix was first proposed in [5]. Correspondingly, a method of evidence accumulation clustering (EAC) based on this theory was proposed for the ensemble clustering problem. Subsequent researches have made various improvements, such as using the technique of normalised edges and matrix completion [29, 45]. In graph partitioning, the graph model and consensus function are usually constructed to partition the graph into multiple parts representing the final cluster. The primary purpose of graph partitioning is to achieve k-way min-cut partitioning, ensuring that the similarity between subgraphs is as tiny as possible [32]. Constructing a graph model is predominantly based on instances (vertices in hypergraph) or clusters (hyperedges in hypergraph) in base clustering. For example, the cluster-based similarity partitioning algorithm (CSPA) considers the local piecewise similarity and constructs a similarity graph as well as a graph partitioning method to perform ensemble clustering [23]. Compared with CSPA, the link-based ensemble clustering constructs a dense graph with the implied similarity between each instance and individual cluster; the clustering possesses a significant effect but needs too many computations [36]. The last type (median partition based algorithms) transforms ensemble clustering into an objective optimisation problem, which finds a median partition most similar to each base clustering by solving the objective function [17]. However, the issue is NP-hard [4]. Fortunately, some deconstructions, such as using expectation maximisation (EM) [40] and weighted consensus clustering (WCC) [33], have been proposed to find approximate solutions. In addition to the common types introduced above, ensemble algorithms based on voting [21], mutual information [20], finite mixture model [3] and other theories [22, 39] are also meaningful research directions in the field of ensemble clustering.

1.2. Motivations

Ensemble clustering is mainly divided into two steps. One is to generate a base clustering pool, for example, running the same clustering algorithm multiple times with different parameters, running various clustering algorithms multiple times, and performing clustering in subspaces. The other step is to select a consensus function, mainly based on the theories such as co-occurrence matrix, graph segmentation, and information entropy. An overview of ensemble clustering algorithms is depicted in Fig. 1.

In the numerous types of ensemble clustering solutions, the pair-wise co-occurrence based algorithms are pretty naive, easy to implement and have played a massive role in ensemble clustering fields. Nevertheless, these algorithms always treat all clusters in the base clustering equally, ignoring the difference of the clusters [35]. Some attempts have been used in cluster weighting to distinguish the effect of different clusters, such as weighting schemes of information entropy [14] and random walk [16]. The authors used related theories to distinguish different clusters and mine implicit relationships between instances. Corresponding experiments proved that it is effective to distinguish different clusters. However, these approaches always try to complete the ensemble clustering without the joining of features, but only the labels of base clusterings, which may lose some vital information implied in data features.

Compared with the algorithms considering base clustering results only, effectively combining base clustering and original features helps further improve the performance of ensemble clustering. Fuzzy-rough sets offer a high degree of flexibility in enabling the vagueness and imprecision present in real-valued data to be simultaneously modelled effectively [12, 38].

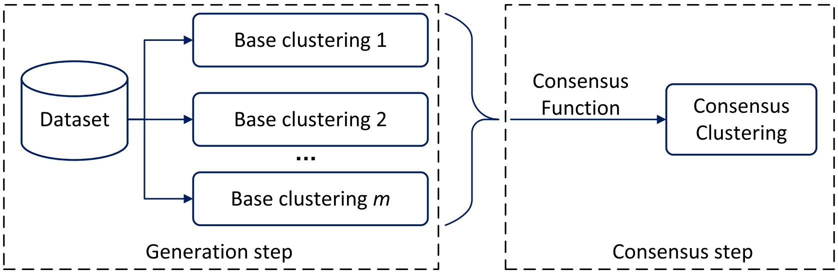

Fig. 1. The outline of ensemble clustering.

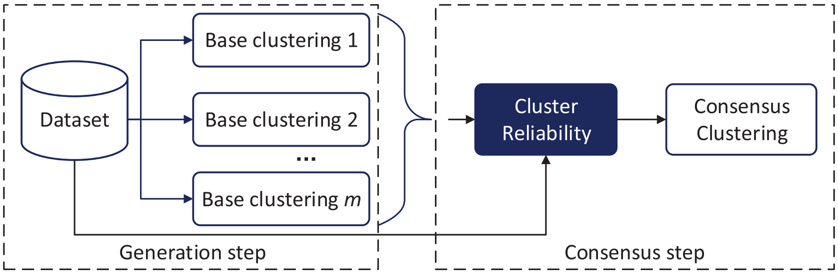

Fig. 2. The motivation of proposed method.

The idea of upper and lower approximation can well depict the membership of instances to each category, which is helpful for measuring the cluster reliability in ensemble clustering. The motivation of the proposed method is described in Fig. 2, and the solid black arrow and blue box are used to illustrate the difference with similar works, which means the joining of original features while distinguishing different cluster reliability.

1.3. Contributions

To distinguish the validity of different clusters and combine the role of features, in this paper, the fuzzy-rough lower approximation is used to induce cluster reliability in all base clusterings. A novel fuzzy-rough induced spectral ensemble clustering (FREC) algorithm is proposed to enhance the performance of pair-wise co-occurrence based ensemble clustering. The contribution of the paper is threefold:

- Proposing the novel idea of cluster reliability through the fuzzy-rough lower approximation of each instance to enable the distinction of diverse cluster significance during clustering;
- Developing a new adjacency matrix based on cluster reliability to effectively enhance the effect of diverse base clusterings and improve the clustering performance;
- Establishing a consensus function and spectral ensemble clustering algorithm with its superiority confirmed through a comparative study and analysis on various benchmark datasets.

The experiment compares eleven state-of-the-art clustering algorithms on ten benchmark datasets, as well as the parallel algorithm that ignores the difference of clusters in base clustering. The result shows that FREC achieves a significant clustering performance. As the ensemble size increases, FREC achieves a superior effect.

The remainder of the paper is structured as follows. The preliminaries of the rough set and fuzzy-rough set are introduced in Section 2. The FREC algorithm is introduced in detail in Section 3. In Section 4, the experimental results are given and analysed. Finally, a summary is presented in Section 5.

2. Preliminaries

This section reviews the mathematical concepts concerning rough set and fuzzy-rough set, which are relevant to the reliability of the cluster developed in this paper.

2.1. Rough set

The study on rough sets theory [13, 41, 49] provides a methodology that can be employed to extract knowledge from a domain in a concise way: it is able to minimise information loss whilst reducing the amount of information involved. Central to rough set theory is the concept of indiscernibility. Let $(\mathbb{U}, \mathbb{A})$ be an information system, where $\mathbb{U}$ is a set of instances and $\mathbb{A}$ is a set of attributes (features) such that $a : \mathbb{U} \rightarrow V_a$ for every $a \in \mathbb{A}$. V_a is the set of values that attribute a may take. For each feature subset $P \subseteq \mathbb{A}$, an associated P-indistinguishable relation can be determined:

$$IND(P) = \{(x, y) \in \mathbb{U}^2 \mid \forall a \in P, a(x) = a(y)\}. \tag{1}$$

Obviously, $IND(P)$ is an equivalence relation on $\mathbb{U}$. The partition of $\mathbb{U}$ determined by $IND(P)$ is herein denoted by $\mathbb{U}/P$ which can be defined such that

$$\mathbb{U}/P = \otimes\{\mathbb{U}/a|a \in P\}. \tag{2}$$

where $\otimes$ is defined as follows for sets V and W:

$$V \otimes W = \{X \cap Y|X \in V, Y \in W, X \cap Y \neq \varnothing\}. \tag{3}$$

For any object $x \in \mathbb{U}$, the equivalence class determined by $IND(P)$, is denoted by $[x]_P$. Let $X \subseteq \mathbb{U}$. X can be approximated using only the information contained in P by constructing the P-lower and P-upper approximations of X [48]:

$$\underline{P}X = \{x \mid [x]_P \subseteq X\}, \tag{4}$$

$$\overline{P}X = \{x \mid [x]_P \cap X \neq \varnothing\}. \tag{5}$$

The pair $\langle \underline{P}X, \overline{P}X\rangle$ is called a rough set. Informally, the former depicts the set of those objects which can be said with certainty to belong to the concept approximated, and the latter is the set of objects which either definitely or possibly belong to the concept approximated. The difference between the upper and lower approximations is the area known as the boundary region that represents the area of uncertainty. If the boundary region is empty, there is no uncertainty regarding the concept which is being approximated and all objects belong to the subset of objects of interest with full certainty.

2.2. Fuzzy-rough set

Fuzzy-rough sets [6, 12, 38] encapsulate the related but distinct concepts of vagueness (for fuzzy sets) and indiscernibility (for rough sets), both of which occur as a result of uncertainty in knowledge. Compared to rough sets, fuzzy-rough sets offer a high degree of flexibility in enabling the vagueness and imprecision present in real-valued data to be simultaneously modelled effectively. In fuzzy-rough sets, the fuzzy lower and upper approximations to approximate a fuzzy concept X can be defined as:

$$\mu_{\underline{R_P}X}(x) = \inf_{y\in\mathbb{U}} \mathcal{I}(\mu_{R_P}(x, y), \mu_X(y)), \tag{6}$$

$$\mu_{\overline{R_P}X}(x) = \sup_{y\in\mathbb{U}} \mathcal{T}(\mu_{R_P}(x, y), \mu_X(y)). \tag{7}$$

Here, $\mathcal{I}$ is a fuzzy implicator and $\mathcal{T}$ is a T-norm. R_P is a T-transitive fuzzy similarity relation induced by the subset of features P:

$$\mu_{R_P}(x, y) = \mathcal{T}_{a\in P}\{\mu_{R_a}(x, y)\}, \tag{8}$$

where $\mu_{R_a}(x, y)$ is the degree to which object x and y are similar for feature a, and may be defined in many ways, for example:

$$\mu_{R_a}(x, y) = \exp(-\frac{(a(x) - a(y))^2}{2{\sigma_a}^2}), \tag{9}$$

$$\begin{aligned}\mu_{R_a}(x, y) = \max(\min(&\frac{(a(y) - (a(x) - \sigma_a))}{(a(x) - (a(x) - \sigma_a))},\\ &\frac{((a(x) + \sigma_a) - a(y))}{((a(x) + \sigma_a) - a(x))}), 0).\end{aligned} \tag{10}$$

Same as their crisp parallels, $\mu_{\underline{R_P}X}(x)$ and $\mu_{\overline{R_P}X}(x)$ indicate the degrees to which the object x must and may belong to the approximated fuzzy concept X, respectively.

3. Fuzzy-rough induced spectral ensemble clustering

3.1. The unacceptable degree of clusters

The validity of a cluster can be well judged by considering the unacceptable degree (UD) of clusters in a base clustering. In multiple base clusterings, if the assignment of a cluster in one base clustering is consistently agreed by other base clusterings, this cluster should play a more critical role in the final consensus clustering. At the same time, if the assignment of a cluster is constantly negated by other base clusterings, the cluster should play a minor role.

For illustration purposes, some formalised descriptions are first introduced below. Let $\mathbb{U} = \{x_i|i \in$

$1, 2, ..., n\}$ be an instances set, x_i is an instance which contains d features. $B = \{\beta_j | j \in 1, 2, ..., m\}$ is a set of base clusterings where $\beta_j = \{\beta_j^k | k \in 1, 2, ..., K\}$ indicates the instances set in the k-th cluster of the j-th base clustering. The degree of x_i belongs to β_j^k with the features set $\mathbb{A}$ can be calculated by the fuzzy lower approximation $\mu_{\underline{R_{\mathbb{A}}}\beta_j^k}(x_i)$.

Since for every fuzzy implicator $\mathcal{I}$, there is $\mathcal{I}(x, 1) = 1$, $\mu_{\underline{R_{\mathbb{A}}}\beta_j^k}(x_i)$ can be simplified into:

$$\begin{aligned} &\mu_{\underline{R_{\mathbb{A}}}\beta_j^k}(x_i) \\ =&\inf_{y\in\mathbb{U}} \mathcal{I}(\mu_{R_{\mathbb{A}}}(x_i, y), \mu_{\beta_j^k}(y)) \\ =&\min\{\min_{y\in\beta_j^k} \left\{\mathcal{I}\left(\mu_{R_{\mathbb{A}}}(x_i, y), 1\right)\right\}, \\ &\min_{y\notin\beta_j^k} \left\{\mathcal{I}\left(\mu_{R_{\mathbb{A}}}(x_i, y), 0\right)\right\}\} \\ =&\min_{y\notin\beta_j^k} \left\{\mathcal{I}\left(\mu_{R_{\mathbb{A}}}(x_i, y), 0\right)\right\}. \end{aligned} \tag{11}$$

As proved in [31], if $\mathcal{I}$ belongs to S-implications, QL-implications or R-implications which enjoys contrapositive symmetry, it is that $\mathcal{I}(x, 0) = \mathcal{N}(x)$, where $\mathcal{N}$ is the strong negator to induce $\mathcal{I}$. In particular, for the classical strong negation $\mathcal{N}_C(x) = 1 - x$, Equation (11) can be further modified to:

$$\begin{aligned} \mu_{\underline{R_{\mathbb{A}}}\beta_j^k}(x_i) &= \min_{y\notin\beta_j^k} \left\{1 - (\mu_{R_{\mathbb{A}}}(x_i, y))\right\} \\ &= 1 - \max_{y\notin\beta_j^k}\{\mu_{R_{\mathbb{A}}}(x_i, y)\}. \end{aligned} \tag{12}$$

Equation (12) implies that the lower approximation of x_i to β_j^k depends on the most similar instance in different clusters, which has a crucial role in ensemble clustering. It indicates that the farther the two clusters are, the greater the lower approximation of each instance to the cluster to which it belongs. At the same time, it means that the distinction between clusters is more obvious, that is, the cluster allocation scheme is more reasonable.

For different base clusterings, the assignment of clusters is distinct, but the data location is fixed, that is, multiple base clusterings are acting on the same dataset. For a specific cluster in one base clustering, the resulting assignment has two cases:

- Another base clustering approves this assignment;
- Another base clustering denies this assignment.

In this paper, a novel concept of UD is proposed to metric the cluster reliability. Here, two exemplar artificial datasets $D1$ (shown in Fig. 3) and $D2$ (shown in Fig. 4) are employed to illustrate the UD of the two cases.

The first case is relatively simple, as shown in Fig. 3, including two exemplar base clusterings β_1 and β_2 in $D1$. For a specifically given cluster (e.g., β_1^1) in base clustering β_1, considering the distribution of this cluster in another base clustering β_2, an obvious fact is that if the particular cluster in β_1 is a subset of one cluster in β_2, the assignment of the cluster (e.g. β_1^1) can be considered to be fully admitted by β_2. At this point, the UD of the specific cluster in β_1 is 0, which means that the objects of the cluster in β_1 meeting the above condition can be divided into one cluster in both base clustering β_1 and β_2.

For the three clusters (β_1^1, β_1^2, β_1^3) of β_1 shown in Fig. 3(a), considering the base clustering β_2, β_1^1 is a subset of β_2^1, and both β_1^2 and β_1^3 are subsets of β_2^2, so the UD is 0 for all three clusters in β_1. It is worth noting that this relationship is not symmetric, that is, the clusters in β_1 are admitted by β_2, which does not mean that the clusters in β_2 are admitted by β_1.

Another situation is shown in Fig. 4. For a particular cluster in β_3, if the cluster objects are split into a plurality of clusters in another base clustering β_4, it can be considered that the specific cluster is not admitted or accepted by β_4. Here, β_3^1 is split into β_4^1 and β_4^2 by β_4, and β_3^2 is split into β_4^3 and β_4^4 by β_4, which means β_4 disagrees with the allocation of β_3^1 and β_3^2. Further, the UD can be well measured by the lower approximation of cluster objects in β_3 to the base clustering β_4.

More specifically, for a specific cluster in a base clustering, considering its position distribution in another base clustering, if the objects of this particular cluster have a more significant lower approximation to the cluster in which the objects relocate in another base clustering, it indicates that the given cluster prefers the allocation of another base clustering. At the same time, it also means the extent of another base clustering does not accept the assignment of the given cluster.

Objects from β_j^k may be located in one or multiple clusters in another base clustering β_l , such indeterminate clusters can be represented by

$$R_{jl}^k = \{\beta_l^s | \beta_j^k \cap \beta_l^s \neq \varnothing, \beta_l^s \in \beta_l\}, l \neq j \tag{13}$$

For the example cluster β_3^1 in Fig. 4(a), the set R_{34}^1 is $\{\beta_4^1, \beta_4^2\}$. Based on the analysis above, the UD γ_{jl}^k

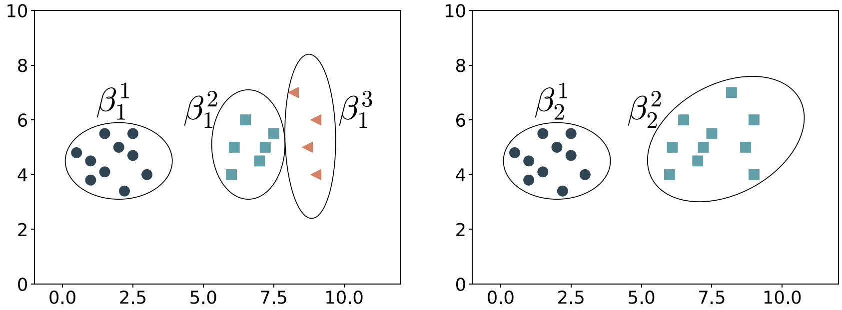

(a) β_1 (b) β_2

Fig. 3. Two exemplar base clusterings β_1 and β_2 in dataset $D1$.

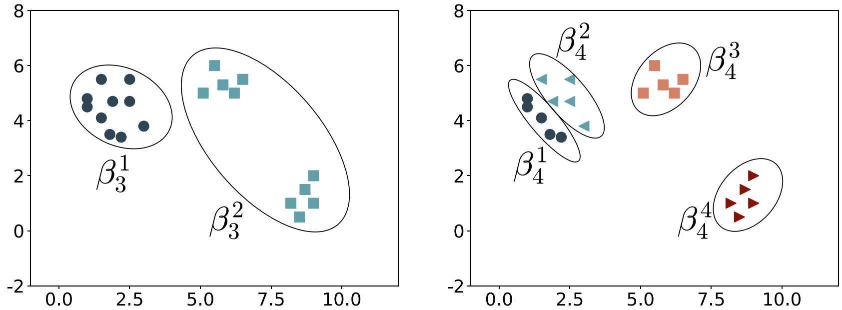

(a) β_3 (b) β_4

Fig. 4. Two exemplar base clusterings β_3 and β_4 in dataset $D2$.

of the cluster β_j^k relative to another base clustering β_l can be defined as:

$$\gamma_{jl}^k = \begin{cases} 0, & |R_{jl}^k| = 1, \\ \frac{1}{|\beta_j^k|} \sum_{\beta_l^s \in R_{jl}^k} \sum_{x_i \in \beta_j^k \cap \beta_l^s} \mu_{\underline{R_{\mathbb{A}}}\beta_l^s}(x_i), & |R_{jl}^k| > 1. \end{cases} \tag{14}$$

where $|R_{jl}^k|$ indicates the number of the clusters in set $|R_{jl}^k|$, and $|\beta_j^k|$ represents the number of the instances in β_j^k.

To illustrate the concepts involved, the objects of the exemplar clusters β_3^1 and β_3^2 in Fig. 4(a) are given in Table 1, the relocated clusters in β_4 are recorded in Table 2.

Take x_1, x_6, x_{11} and x_{16} as an example (located in diverse clusters in β_4), the respective lower approximation of the above four objects to β_4 are obtained by using the Algebraic T-norm $\mathcal{T}_P(a,b) = ab$ and the fuzzy similarity function (9):

$$\begin{aligned} x_1 &\in \beta_4^1 &\Rightarrow\ & \mu_{\underline{R_{\mathbb{A}}}\beta_4^1}(x_1) = 0.05, \\ x_6 &\in \beta_4^2 &\Rightarrow\ & \mu_{\underline{R_{\mathbb{A}}}\beta_4^2}(x_6) = 0.05, \\ x_{11} &\in \beta_4^3 &\Rightarrow\ & \mu_{\underline{R_{\mathbb{A}}}\beta_4^3}(x_{11}) = 0.91, \\ x_{16} &\in \beta_4^4 &\Rightarrow\ & \mu_{\underline{R_{\mathbb{A}}}\beta_4^4}(x_{16}) = 0.94. \end{aligned}$$

Through further calculations, the lower approximation of all objects in β_3 to the base clustering β_4 are shown in Table 3.

Then, the UD of β_3^1 and β_3^2 to base clustering β_4 is computed by Equation (14), there is

$$\gamma_{34}^1 = \frac{0.05+0.05+0.07+0.06+0.10+0.05+0.11+0.10+0.19+0.07}{10} = 0.09$$

$$\gamma_{34}^2 = \frac{0.91+0.90+0.96+0.86+0.91+0.94+0.86+0.91+0.97+0.95}{10} = 0.92$$

Table 1
Two exemplar clusters in Fig. 4(a)

Cluster	Sample	x_1	x_2	x_3	x_4	x_5	x_6	x_7	x_8	x_9	x_{10}
β_3^1	x-axis	1.0	1.0	1.5	2.2	1.8	1.9	2.5	1.5	2.5	3.0
	y-axis	4.5	4.8	4.1	3.4	3.5	4.7	4.7	5.5	5.5	3.8
Cluster	Sample	x_{11}	x_{12}	x_{13}	x_{14}	x_{15}	x_{16}	x_{17}	x_{18}	x_{19}	x_{20}
β_3^2	x-axis	5.8	5.1	5.5	6.2	6.5	8.2	9.0	8.7	8.5	9.0
	y-axis	5.3	5.0	6.0	5.0	5.5	1.0	2.0	1.5	0.5	1.0

Table 2
Relocated cluster of the objects in β_3^1 and β_3^2

Sample (β_3^1)	x_1	x_2	x_3	x_4	x_5	x_6	x_7	x_8	x_9	x_{10}
Relocated cluster			β_4^1					β_4^2		
Sample (β_3^2)	x_{11}	x_{12}	x_{13}	x_{14}	x_{15}	x_{16}	x_{17}	x_{18}	x_{19}	x_{20}
Relocated cluster			β_4^3					β_4^4		

Table 3
Lower approximation of β_3^1 and β_3^2 to the base clustering β_4

Cluster	Relocation	x_1	x_2	x_3	x_4	x_5	x_6	x_7	x_8	x_9	x_{10}
β_3^1	β_4^1	0.05	0.05	0.07	0.06	0.10	-	-	-	-	-
	β_4^2	-	-	-	-	-	0.05	0.11	0.10	0.19	0.07
Cluster	Relocation	x_{11}	x_{12}	x_{13}	x_{14}	x_{15}	x_{16}	x_{17}	x_{18}	x_{19}	x_{20}
β_3^2	β_4^3	0.91	0.90	0.96	0.86	0.91	-	-	-	-	-
	β_4^4	-	-	-	-	-	0.94	0.86	0.91	0.97	0.95

Considering the ground distribution of β_3^1 and β_3^2 in Fig. 4, apparently, the allocation scheme of β_3^1 is more reasonable, with a lower UD of 0.09. While β_3^2 groups the objects with an enormous difference, the UD is 0.92. The result shows that the UD acquired is consistent with the actual situation of the clusters.

Further, the global UD γ_j^k of a cluster in β_j to the remaining $m-1$ base clustering can be calculated as follows:

$$\gamma_j^k = \frac{1}{m-1} \sum_{l \neq j} \gamma_{jl}^k, \quad l = 1, 2, ..., m. \tag{15}$$

The unacceptable degree computing (UDC) algorithm is outlined in Algorithm 1. Given the inputs $\mathbb{U}$ and m, the first step is to initialise the set Γ empty and generate m base clusterings by any constructed method, such as repeating k-means m times and using diverse results from multiple clustering algorithms [34]. The loop in Lines 3 to 14 traverses each cluster in all base clusterings and computes the UD. Specifically, β_j^k represents the current cluster to calculate UD, and β_l indicates any cluster in the base clusterings set except β_j. Mean($\cdot$) defines an average process, and all computed UD is stored in Γ. Finally, in Line 15, the Γ is returned for subsequent calculations.

3.2. Defining the co-association matrix

The co-association matrix is obtained by summing and averaging a series of co-occurrence matrices, and it represents the frequency with which two objects co-occur in multiple base clusterings. Each base clustering β_j produces a separate co-occurrence matrix, which can be expressed as

$$O_j = \{o_{ih}^j\}_{n \times n}, \tag{16}$$

where o_{ih}^j represents whether x_i and x_h co-occur in β_j. Let $C_j(x_i)$ indicate the serial number of the cluster to which x_i belongs in the j-th base clustering, o_{ih}^j can be denoted by

$$o_{ih}^j = \begin{cases} 1, & C_j(x_i) = C_j(x_h), \\ 0, & C_j(x_i) \neq C_j(x_h). \end{cases} \tag{17}$$

Further, the co-association matrix can be expressed as

$$A = \{a_{ih}\}_{n \times n}, \tag{18}$$

where a_{ih} is calculated by

$$a_{ih} = \frac{1}{m} \sum_{j=1}^{m} o_{ih}^j. \tag{19}$$

	x_1	x_2	…	x_6	…	x_{20}
x_1	1	1	…	1	…	0
x_2	1	1	…	1	…	0
…	…	…	…	0	…	…
x_6	1	1	0	1	…	0
…	…	…	…	…	…	…
x_{20}	0	0	0	0	…	1

O_3

+

	x_1	x_2	…	x_6	…	x_{20}
x_1	1	1	…	0	…	0
x_2	1	1	…	0	…	0
…	…	…	…	0	…	…
x_6	0	0	0	1	…	0
…	…	…	…	…	…	0
x_{20}	0	0	0	0	0	1

O_4

Mean

	x_1	x_2	…	x_6	…	x_{20}
x_1	1	1	…	0.5	…	0
x_2	1	1	…	0.5	…	0
…	…	…	…	0	…	…
x_6	0.5	0.5	0	1	…	0
…	…	…	…	…	…	…
x_{20}	0	0	0	0	…	1

A

Fig. 5. Matrices O_3, O_4 and A of the example in Fig. 4.

	x_1	x_2	…	x_6	…	x_{20}
x_1	1	0.91	…	0.91	…	0
x_2	0.91	1	…	0.91	…	0
…	…	…	…	0	…	…
x_6	0.91	0.91	0	1	…	0
…	…	…	…	…	…	…
x_{20}	0	0	0	0	…	1

$\tilde{O}_3$

+

	x_1	x_2	…	x_6	…	x_{20}
x_1	1	1	…	0	…	0
x_2	1	1	…	0	…	0
…	…	…	…	0	…	…
x_6	0	0	0	1	…	0
…	…	…	…	…	…	0
x_{20}	0	0	0	0	0	1

$\tilde{O}_4$

Mean

	x_1	x_2	…	x_6	…	x_{20}
x_1	1	0.96	…	0.46	…	0
x_2	0.96	1	…	0.46	…	0
…	…	…	…	0	…	…
x_6	0.46	0.46	0	1	…	0
…	…	…	…	…	…	…
x_{20}	0	0	0	0	…	1

$\tilde{A}$

Fig. 6. Redefined Matrices $\tilde{O}_3$, $\tilde{O}_4$ and $\tilde{A}$ of the example in Fig. 4.

Given the exemplar clusters in Fig. 4 and corresponding coordinates in Table 1, the matrices O_3, O_4 and A are recorded in Fig. 5. Take x_1 and x_6 as an example (marked as a blue box) :

$$C_3(x_1) = C_3(x_6) \quad \Rightarrow \quad o_{16}^3 = 1,\ o_{61}^3 = 1,$$
$$C_4(x_1) \neq C_4(x_6) \quad \Rightarrow \quad o_{16}^4 = 0,\ o_{61}^4 = 0.$$

Then, the elements a_{16} and a_{61} of A are calculated by

$$o_{16}^3 = 1, o_{16}^4 = 0 \ \Rightarrow\ a_{16} = (1+0)/2 = 0.5,$$
$$o_{61}^3 = 1, o_{61}^4 = 0 \ \Rightarrow\ a_{61} = (1+0)/2 = 0.5.$$

A higher UD for a cluster indicates that other base clusterings are more likely to disapprove of the cluster's allocation scheme. At this point, the role of the cluster should be weakened. Otherwise, the function of the cluster should be reinforced. Therefore, the reliability of a cluster can be described as a decreasing function of the UD. In this paper, the reliability of the k-th cluster in β_j is defined as

$$\mu_j^k = 1 - \gamma_j^k. \tag{20}$$

Similar to Equations (16), (17), (18) and (19), the redefined co-occurrence matrix $\tilde{O}_j$ and co-association matrix $\tilde{A}$ are expressed as

$$\tilde{O}_j = \{\tilde{o}_{ih}^j\}_{n\times n}, \tag{21}$$

$$\tilde{A} = \{\tilde{a}_{ih}\}_{n\times n}, \tag{22}$$

where

$$\tilde{o}_{ih}^j = \begin{cases} \mu_j^k, & C_j(x_i) = C_j(x_h), \\ 0, & C_j(x_i) \neq C_j(x_h). \end{cases} \tag{23}$$

$$\tilde{a}_{ih} = \frac{1}{m}\sum_{j=1}^{m} \tilde{o}_{ih}^j. \tag{24}$$

Again, for the example of x_1 and x_6,

$$C_3(x_1) = C_3(x_6) \ \Rightarrow\ \tilde{o}_{16}^3 = 0.91,\ \tilde{o}_{61}^3 = 0.91,$$
$$C_4(x_1) \neq C_4(x_6) \ \Rightarrow\ \tilde{o}_{16}^4 = 0,\ \tilde{o}_{61}^4 = 0.$$

Then, the elements $\tilde{a}_{16}$ and $\tilde{a}_{61}$ of $\tilde{A}$ are computed by

$$\left.\begin{array}{l} \tilde{o}_{16}^3 = 0.91 \\ \tilde{o}_{16}^4 = 0 \end{array}\right\} \ \Rightarrow\ \tilde{a}_{16} = (0.91+0)/2 = 0.46,$$

Algorithm 1 Unacceptable Degree Computing (UDC)

UDC ($\mathbb{U}$, m)
Input:
  $\mathbb{U}$, input space containing n objects,
  m, number of base clusterings.
Output:
  Γ, set of unacceptable degree of all clusters,
  B, set of base clusterings.
Initialise: $\Gamma = \varnothing$.
$B \leftarrow$ Generate m base clustering.
foreach β_j in B **do**
  foreach β_j^k in β_j **do**
    $S = \varnothing$
    foreach β_l in $\{B - \beta_j\}$ **do**
      $R_{jl}^k \leftarrow$ Equation (13)
      $\gamma_{jl}^k \leftarrow$ Equation (14)
      $S = S \cup \gamma_{jl}^k$
    end
    $\gamma_j^k = \text{Mean}(S)$
    $\Gamma = \Gamma \cup \gamma_j^k$
  end
end
return Γ, B

$$\left.\begin{array}{l}\tilde{o}_{61}^3 = 0.91\\ \tilde{o}_{61}^4 = 0\end{array}\right\} \Rightarrow \tilde{a}_{61} = (0.91 + 0)/2 = 0.46.$$

The matrices $\tilde{O}_3$, $\tilde{O}_4$ and $\tilde{A}$ of the exemplar clusters in Fig. 4 are recalculated and shown in Fig. 6.

The co-association matrix construction (CMC) algorithm is detailed in Algorithm 2. Firstly, the initialised step is performed. Lines 2 to 17 represent the overall process, including the main loop to identify the co-occurrence and co-association matrices. Note that all matrices are calculated only for upper triangular due to the symmetry. In Line 15, the lower triangular matrix of $\tilde{A}$ directly takes the values from the existing result in Line 14, which can significantly diminish unnecessary calculations. The final co-association matrix $\tilde{A}$ is output in Line 18.

3.3. Consensus function

A mapping from a set of clusterings to a single final clustering is called a consensus function. Considering the superior performance of spectral clustering in complex shapes and cross data, in this paper, the optimised co-association matrix is used in the spectral method to acquire the consensus result.

Algorithm 2 Co-Association Matrix Construction (CMC)

CMC ($\mathbb{U}$, Γ, B)
Input:
  $\mathbb{U}$, input space containing n objects,
  Γ, set of unacceptable degree of all clusters,
  B, set of base clusterings.
Output: $\tilde{A}$, co-association matrix.
1: **Initialise**: $\tilde{A} = \{\tilde{a}_{ih}\}_{n\times n}(\tilde{a}_{ih} = 1)$, $\tilde{O}_j = \{\tilde{o}_{ih}^j\}_{n\times n}(\tilde{o}_{ih}^j = 0)$.
2: **foreach** $i = 1$ to n **do**
3:   **foreach** $h = i + 1$ to n **do**
4:     $Q = \varnothing$
5:     **foreach** β_j in B **do**
6:       **if** $C_j(x_i) \neq C_j(x_h)$ **then** $\tilde{o}_{ih}^j = 0$
7:       **else**
8:         $k = C_j(x_i)$
9:         $\mu_j^k = 1 - \gamma_j^k$
10:         $\tilde{o}_{ih}^j = \mu_j^k$
11:       **end**
12:       $Q = Q \cup \tilde{o}_{ih}^j$
13:     **end**
14:     $\tilde{a}_{ih} = \text{Mean}(Q)$
15:     $\tilde{a}_{hi} = \tilde{a}_{ih}$
16:   **end**
17: **end**
18: **return** $\tilde{A}$

Given a graph model $G = (V, L)$, where V indicates the vertexes set and L represents the links set. Its adjacency matrix can be constructed in various ways, such as considering the neighbours or defining the distance threshold. Let the objects in $\mathbb{U}$ be the vertexes in the graph, the adjacency matrix can be expressed as $\tilde{A}$. It means that if a_{ih} is 0, there is no edge connection between x_i and x_h. Otherwise, the edge exists and the similarity is a_{ih}. From this, the diagonal matrix D can be expressed by

$$D = \{d_{ih}\}_{n\times n}, \tag{25}$$

where

$$d_{ih} = \begin{cases} 0, & i \neq h, \\ \sum_{q=1}^{n} \tilde{a}_{iq}, & i = h. \end{cases} \tag{26}$$

The Laplacian matrix L of the graph G can be further defined as

$$L = D - \tilde{A}. \tag{27}$$

Normalisation makes the diagonal entries of the Laplacian matrix to be all units and scales off-diagonal entries correspondingly. In this case, the normalised Laplacian matrix L_{nor} is defined as

$$L_{nor} = D^{-\frac{1}{2}} L D^{-\frac{1}{2}}. \tag{28}$$

The components of the eigenvectors corresponding to the smallest eigenvalues of the graph Laplacian can be used for meaningful clustering [42]. In Equation (28), the eigenvectors corresponding to the first K smallest eigenvalues of L_{nor} will be used in an independent clustering algorithm, generally k-means, due to its speed and efficiency.

As summarised in Algorithm 3, D and L_{nor} are computed sequentially in Lines 2 to 6. EV$(\cdot)$ in Line 7 represents a function that generates the first K eigenvectors, and k-means$(\cdot)$ in Line 8 indicates a fast clustering algorithm detailed in [34]. Finally, in Line 9, $\mathcal{R}$ is used to return the consensus clustering result.

Algorithm 3 Consensus Spectral Clustering (CSC)

CSC $(\tilde{A}, K)$
Input:
$\tilde{A}$, co-association matrix,
K, number of clusters.
Output: $\mathcal{R}$, consensus result.
1: **Initialise**: $D = \{d_{ih}\}_{n\times n}$ $(d_{ih} = 0)$.
2: **foreach** $i = 1$ to n **do**
3: $\quad d_{ii} = \sum_{q=1}^{n} \tilde{a}_{iq}$
4: **end**
5: $L = D - \tilde{A}$
6: $L_{nor} = D^{-\frac{1}{2}} L D^{-\frac{1}{2}}$
7: $F \leftarrow \mathrm{EV}(L_{nor})$
8: $\mathcal{R} \leftarrow k\text{-means}(F, K)$
9: **return** $\mathcal{R}$

3.4. *Fuzzy-rough induced spectral ensemble clustering*

According to the description of the above three subsections, the overall fuzzy-rough induced spectral ensemble clustering is depicted in Algorithm 4. Given a dataset $\mathbb{U}$, the number of base clusterings m and the actual clusters number K. Algorithm 1 is first executed to generate the UD set Γ of all clusters and the set of base clusterings B in Line 1. Further, the result returned by Algorithm 1 is combined with the dataset $\mathbb{U}$ as the parameters of Algorithm 2 to calculate the co-association matrix $\tilde{A}$. Finally, the matrix $\tilde{A}$ is used in the consensus spectral clustering (CSC) to generate the final clustering result $\mathcal{R}$.

Algorithm 4 Fuzzy-Rough Induced Spectral Ensemble Clustering (FREC)

FREC $(\mathbb{U}, m, K)$
Input:
$\mathbb{U}$, input space containing n objects,
m, number of base clusterings,
K, number of clusters.
Output: $\mathcal{R}$, consensus result.
1: $\Gamma, B =$ **UDC**$(\mathbb{U}, m)$ //Algorithm 1
2: $\tilde{A} =$ **CMC**$(\mathbb{U}, \Gamma, B)$ //Algorithm 2
3: $\mathcal{R} =$ **CSC**$(\tilde{A}, K)$ //Algorithm 3
4: **return** $\mathcal{R}$

4. Experimental evaluation

This section presents the experimental evaluation of FREC and other algorithms on ten popular datasets contained in UCI[1] repository. For convenience, datasets *Cardiotocography*, *Image Segmentation*, and *Steel Plates Faults* are represented by abbreviations *Cardio*, *IS*, and *SPF*, respectively. After introducing the experimental setup, the results and discussion are divided into five parts. Section 4.2 analyses the tendency of clustering effect as the number of ensembles increases. To test the impact of cluster reliability induced by fuzzy-rough lower approximation, Section 4.3 compares the effect of FREC and the original parallel algorithm EAC on all benchmark datasets. Besides, the average result of 100 base clusterings is also used to compare and validate the ensemble performance. In Sections 4.4 and 4.5, a detailed analysis of FREC and other state-of-the-art clustering algorithms is reported. Finally, the time complexity of the proposed method and running time of each algorithm are analysed in Section 4.6.

4.1. *Experimental setup*

In the experimental investigation, all datasets are normalised first. Homogeneity score (HS) and normalised mutual info (NMI) are used to evaluate the performance of the separate clustering method [10, 15]. The base clustering pool B in Algorithm 1 is generated by running the k-means method 100 times,

[1] https://archive.ics.uci.edu/ml/datasets.php

Table 4
Benchmark datasets used for evaluation

Datasets	Attributes	Class	Size
Heart	13	2	270
Cleveland	13	5	297
Dermatology	34	6	358
Movement	90	15	360
Appendicitis	7	2	106
Led7digit	7	10	500
Mammographic	5	2	830
Cardio	21	10	2126
IS	19	7	2130
SPF	27	7	1941

where the K is randomly selected from the interval $[2, \sqrt{n}]$, in line with [14]. In Section 4.2, the ensemble size increases sequentially from 10 to 100 with a step size of 10. Meanwhile, each ensemble algorithm of a specific size is run 100 times, and the results are averaged. Considering the excellent results of ensemble clustering at larger ensemble number, ensemble size is set to 100 for all ensemble methods in Sections 4.3 and 4.4. At the same time, for a fair comparison, the different algorithms are run 100 times to get the average results.

Ten state-of-the-art ensemble clustering algorithms, namely, locally weighted evidence accumulation (LWEA) [14], locally weighted graph partitioning (LWGP) [14], probability trajectory accumulation (PTA) [16], probability trajectory based graph partitioning (PTGP) [16], ensemble clustering by propagating cluster-wise similarities with hierarchical consensus function (ECPCS-HC) [18], ensemble clustering by propagating cluster-wise similarities with meta-cluster-based consensus function (ECPCS-MC) [18], evidence accumulation clustering (EAC) [5], weighted evidence accumulation clustering (WEAC) [15], graph partitioning with multi-granularity link analysis (GPMGLA) [15], and spectral ensemble clustering (SEC) [26] are selected to compare the ensemble performance of FREC. Moreover, two other non-ensemble state-of-the-art clustering methods, deep temporal clustering representation (DTCR) [37] and robust temporal feature network (RTFN) [50] are also used to compare the performance of the newly proposed method. For FREC, Łukasiewicz t-norm and Equation (9) are used to calculate the fuzzy similarity. As for other compared algorithms, there is no extra parameter for EAC, and the specific parameters of the remaining methods are set according to the recommendations or optimal values given in the corresponding papers. More specifically, the core settings are listed as follows.

– LWEA, LWGP: $\theta = 0.4$;
– PTA, PTGP: $K = \sqrt{N}/2, T = \sqrt{N}/2$ where N indicates the number of the graph nodes;
– ECPCSHC, ECPCSMC: $t = 20$;
– WEAC, GPMGLA: $\alpha = 0.5, \beta = 2$;
– SEC: $\mu = 1$;
– DTCR: $m_1 = 100, m_2 = 50, m_3 = 50, \lambda = 1e-1, lr = 1e-4$;
– RTFN: CNN channel = 128, kernel size = 11,
$l_{rate}(0) = 0.01, d_{rate} = 0.1$.

4.2. The influence of ensemble size

Figures 7 and 8 show the experimental results for different ensemble sizes, including two indexes of HS and NMI on ten benchmark datasets. The various contrastive algorithms use different colours, lines and markers, as the legend details. Apparently, for the proposed FREC, as the ensemble size increases, the results on nearly all datasets deliver an upward trend regardless of the evaluation criteria, which is in line with the objective of ensemble methods. More specifically, considering HS, FREC shows significantly superior performance on datasets *Heart*, *Appendictis*, *Led7digit* and *Mammographic*, i.e. no matter how large the ensemble size is, FREC can invariably outperform the other ten ensemble techniques. For *Dermatology* and *SPF*, if the ensemble size is less than 40, the effect of FREC is slightly lower than that of GPMGLA and LWEA, respectively, but exceeds that of the other nine methods. If the ensemble size is more significant than 40, the proposed method performs superiorly, outperforming all different ways. While *Cleveland*, *Cardio*, and *IS* are not optimal in all ensemble sizes, FREC can always exceed most comparison approaches and always shows the best or second best performance if the ensemble size is maximum. Finally, for *Movement*, as the ensemble size increases, the performance of FREC tends to stabilise rapidly, and there is no apparent transformation trend. However, it can still surpass almost all contrastive algorithms.

While using the evaluation index NMI, the results are resemblance. For *Heart*, *Appendictis*, *Led7digit* and *Mammographic*, FREC can accomplish best values at any ensemble size, and the performance grows and stabilises as the ensemble size boosts. Regarding *Cardio*, although FREC is slightly lower than some methods if the ensemble size is less than 90, FREC still performs satisfactorily if the ensemble size is the largest, which ranks third. The curves of FREC

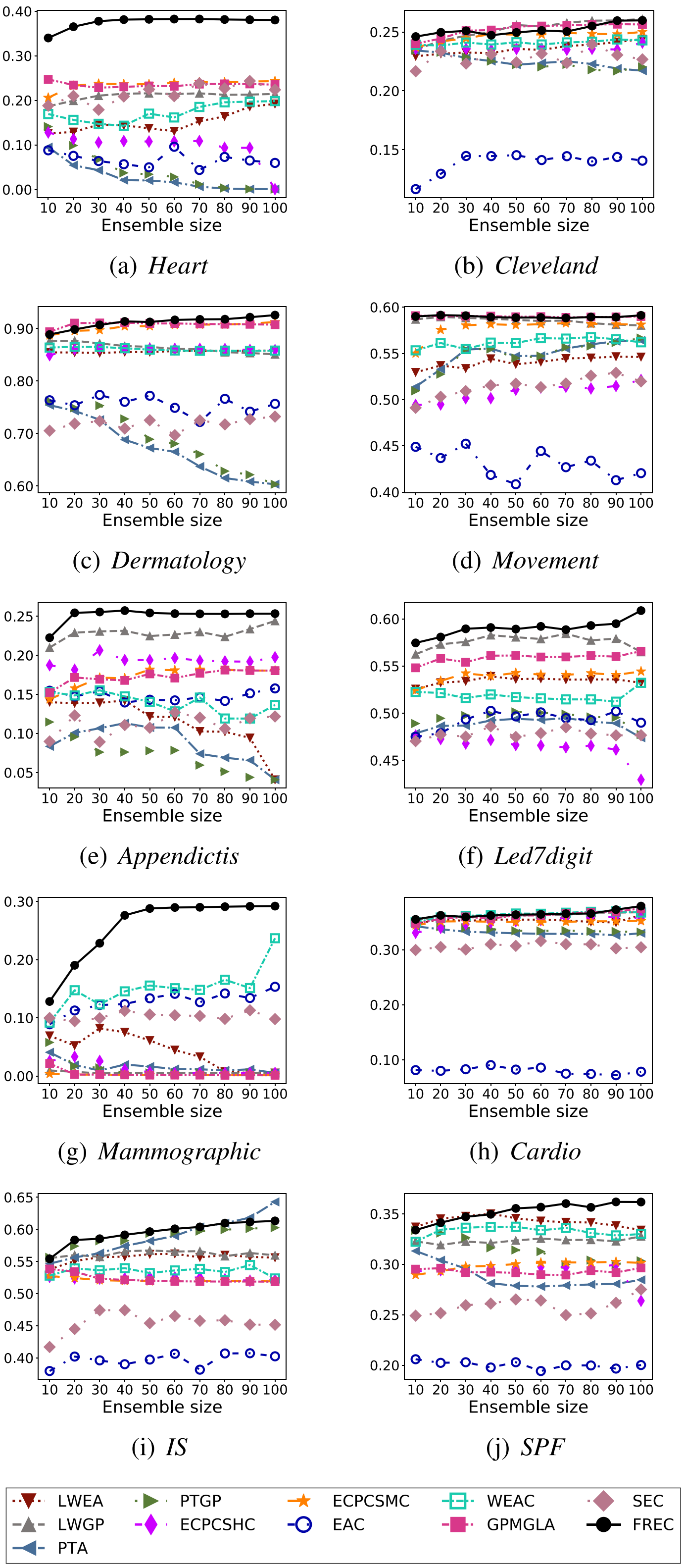

Fig. 7. HS results with the ensemble size.

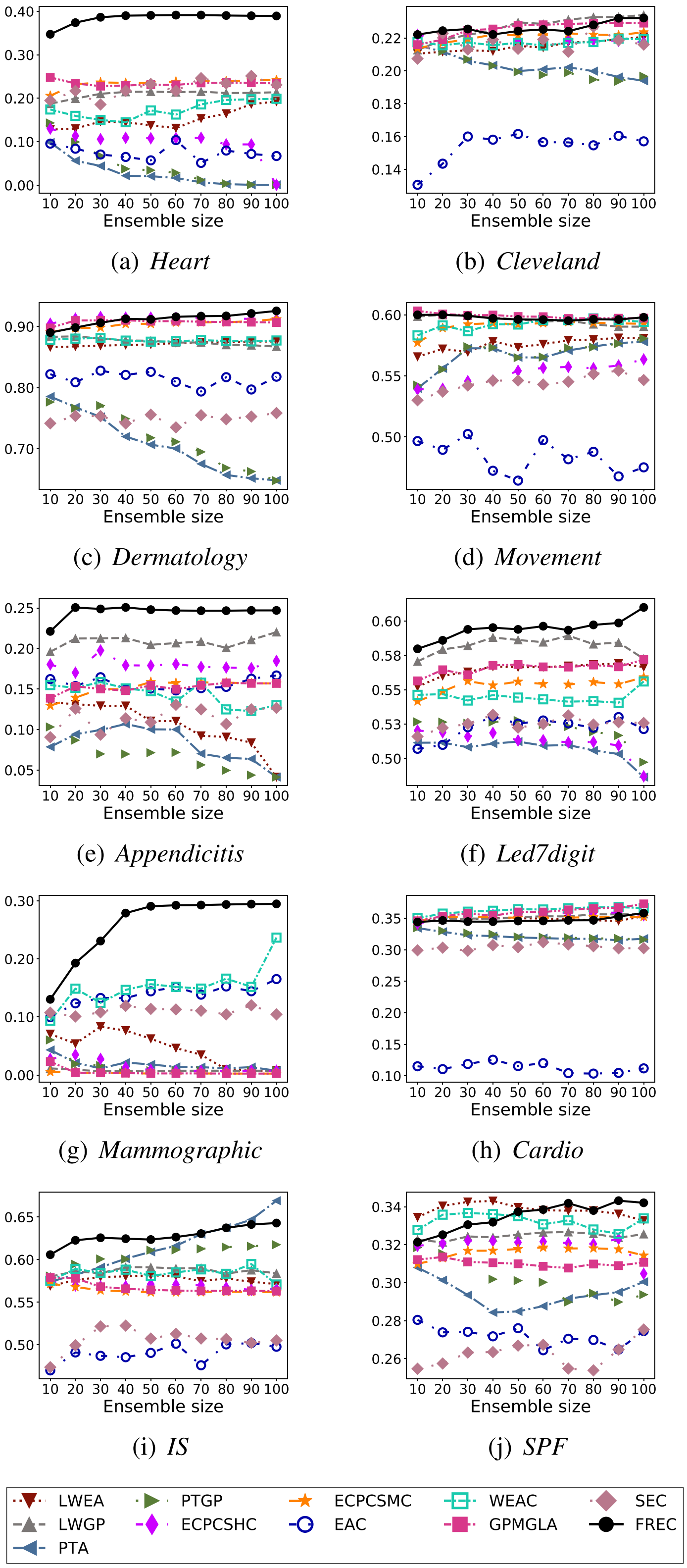

Fig. 8. NMI results with the increased ensemble size.

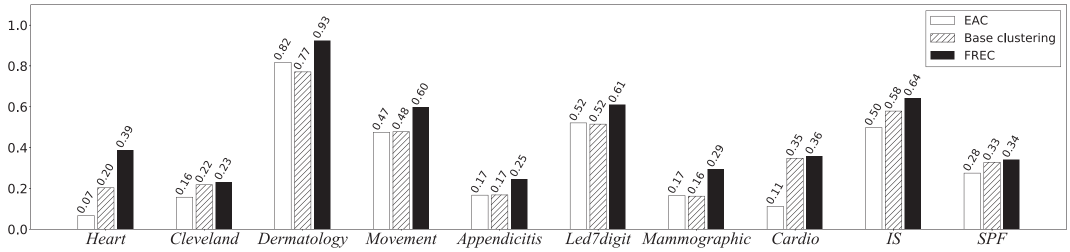

Fig. 9. NMI results of FREC versus the parallel EAC and base clustering.

may be slightly lower for the remaining datasets than individual algorithms at a particular ensemble size. Still, FREC can consistently achieve better results, especially at the largest ensemble size.

4.3. Comparison to the parallel EAC and base clustering

The algorithm EAC, which means the original co-association based ensemble scheme that does not consider cluster reliability, always conducts poorly in both HS and NMI. As exampled in Fig. 7(b), 7(d), 7(h) and 7(iFor the three clusters), EAC conveys the worst effect regardless of the ensemble size by comparing the other ten ensemble algorithms. To more comprehensively recognise the effect of using the cluster reliability induced by fuzzy-rough set, this part compares FREC and the parallel EAC in detail in the form of a histogram.

Since all ensemble strategies primarily achieve more satisfactory results at larger ensemble sizes, FREC and EAC use the pool containing 100 base clusterings. Moreover, both algorithms are run 100 times to acquire the average results. In addition, the algorithms in the base clustering pool (k-means) are also averaged to compare the ensemble performance.

Without overloading similar results, the NMI is used to report the experiment evaluation. As shown in Fig. 9, FREC consistently achieves a better clustering effect relative to the parallel EAC and base clustering on all datasets. Especially for *Heart*, *Dermatology*, *Movement* and *Mammographic*, FREC reports the best clustering results while achieving a satisfactory improvement, illustrating the advantage which considers the cluster reliability and the superiority of FREC.

4.4. Comparison to other clustering algorithms

In order to comprehensively evaluate the performance of the proposed algorithm, experimental comparisons are carried out against the other eleven state-of-the-art methods. The results are summarised in Tables 5 and 6. Note that the results of EAC have been analysed in Section 4.3 and will not be repeated in this part.

Recall reported results, ensemble algorithms always work best using more ensemble size. Thus, all comparison ensemble methods employ the results with an ensemble size of 100, and the average and best results for each dataset are shown in columns Ave and Best, respectively. To describe the experimental results more obviously, the best results are highlighted in bold. Moreover, the second best results are highlighted with an underline to make the information in the table easier to follow.

Considering the metric HS, FREC achieves optimal average performance relative to the other eleven algorithms in most datasets, including *Heart*, *Dermatology*, *Movement*, *Leg7digit* and *SPF*. As for the results in column Best, although a bit inferior to one or two approaches occasionally, FREC is the best or second best in most cases. For the remaining datasets, the average performance of FREC is slightly lower than individual algorithms. Still, FREC shows a satisfactory clustering effect compared with the other techniques.

Now, take an observation of the evaluation NMI, the clustering result is highly analogous to HS. For datasets *Heart*, *Cleveland*, *Dermatology*, *Movement*, *Appendicitis*, *Leg7digit*, *Mammographic* and *SPF*, the proposed method can consistently surpass most contrasting approaches. For dataset *IS*, consistent with the HS, FREC is slightly inferior to PTA, ranking second in all ensemble methods. The main difference from HS is the dataset *Cardio*. FREC is slightly lower than WEAC and GPMLGA by 0.008 and 0.015, respectively. Nevertheless, compared with the remaining algorithms, FREC still shows excellent performance.

In general, the average and best results of FREC are equal in most cases, which means that the FREC is

Table 5
HS results of FREC versus other ensemble algorithms

Dataset	*Heart*		*Cleveland*		*Dermatology*		*Movement*		*Appendicitis*	
Algorithm	Ave	Best	Ave	Best	Ave	Best	Ave	Best	Ave	Best
LWEA	0.192 v	0.192	0.244 v	0.244	0.858 v	0.858	0.546 v	0.546	0.041 v	0.041
LWGP	0.214 v	0.214	0.260 v	0.260	0.851 v	0.851	0.580 v	**0.594**	0.244 v	0.245
PTA	0.001 v	0.001	0.217 v	0.217	0.603 v	0.603	0.564 v	0.564	0.041 v	0.041
PTGP	0.001 v	0.001	0.220 v	0.220	0.603 v	0.603	0.567 v	0.573	0.041 v	0.041
ECPCSHC	0.001 v	0.001	0.241 v	0.241	0.859 v	0.859	0.521 v	0.521	0.198 v	0.198
ECPCSMC	0.243 v	0.243	0.250 v	0.250	<u>0.912</u> v	0.912	0.581 v	0.584	0.180 v	0.180
WEAC	0.198 v	0.198	0.243 v	0.243	0.858 v	0.858	0.562 v	0.562	0.136 v	0.136
GPMGLA	0.235 v	0.235	0.256 v	0.256	0.907 v	0.907	<u>0.590</u> v	0.590	0.180 v	0.180
SEC	0.224 v	**0.380**	0.227 v	0.227	0.732 v	<u>0.923</u>	0.520 v	0.584	0.122 v	0.154
DTCR	0.288 v	0.288	0.250 v	0.260	0.851 v	0.851	0.460 v	0.460	**0.298** *	**0.298**
RTFN	<u>0.375</u> v	0.375	**0.270** *	**0.270**	0.880 v	<u>0.923</u>	0.558 v	0.558	0.248 v	0.248
FREC	**0.380**	**0.380**	<u>0.261</u>	<u>0.261</u>	**0.926**	**0.926**	**0.591**	<u>0.591</u>	<u>0.253</u>	<u>0.253</u>
Summary	(11/0/0)		(10/0/1)		(11/0/0)		(11/0/0)		(10/0/1)	

Dataset	*Led7digit*		*Mammographic*		*Cardio*		*IS*		*SPF*	
Algorithm	Ave	Best	Ave	Best	Ave	Best	Ave	Best	Ave	Best
LWEA	0.532 v	0.532	0.005 v	0.005	0.363 v	0.363	0.556 v	0.556	0.334 v	0.334
LWGP	0.565 v	0.566	0.005 v	0.005	0.368 v	**0.382**	0.560 v	0.610	0.328 v	0.357
PTA	0.474 v	0.474	0.005 v	0.005	0.330 v	0.330	**0.643** *	**0.643**	0.285 v	0.285
PTGP	0.477 v	0.507	0.005 v	0.005	0.332 v	0.363	0.603 v	<u>0.633</u>	0.303 v	0.341
ECPCSHC	0.429 v	0.429	0.005 v	0.005	0.357 v	0.357	0.521 v	0.521	0.264 v	0.264
ECPCSMC	0.544 v	0.545	0.001 v	0.001	0.352 v	0.356	0.519 v	0.519	0.301 v	0.301
WEAC	0.532 v	0.532	0.237 v	0.237	0.368 v	0.368	0.524 v	0.524	0.330 v	0.330
GPMGLA	0.566 v	0.566	0.001 v	0.001	0.375 v	0.375	0.519 v	0.519	0.296 v	0.296
SEC	0.477 v	0.554	0.098 v	0.289	0.304 v	0.364	0.452 v	0.629	0.275 v	<u>0.376</u>
DTCR	0.500 v	0.500	**0.300** *	**0.300**	0.330 v	0.330	0.535 v	0.535	0.260 v	0.260
RTFN	<u>0.575</u> v	<u>0.575</u>	0.290 v	0.290	**0.380** *	<u>0.380</u>	0.593 v	0.593	<u>0.351</u> v	0.351
FREC	**0.609**	**0.609**	<u>0.292</u>	<u>0.292</u>	<u>0.379</u>	<u>0.380</u>	<u>0.613</u>	0.613	**0.362**	**0.380**
Summary	(11/0/0)		(10/0/1)		(10/0/1)		(10/0/1)		(11/0/0)	

relatively stable and the results are less serendipitous. At the same time, regardless of the average or best results, FREC always achieves the most significant or second best effect, which illustrates the rationality of the research in this paper.

4.5. Statistical analysis

Paired t-test is used throughout the present experimental studies to show any statistically significant differences between different approaches. This helps ensure that the results are not obtained by chance. The t-test results are summarised at the end of each table, counting the number of statistically better(v), equivalent(space) or worse(*) cases for FREC in comparison to each algorithm. In all experiments reported, the threshold of significance is set to 0.05. For example, in Table 6, (11/0/0) in the column *Heart* indicates that the clustering performance returned by FREC performs better than other ensemble methods in eleven cases, equivalently well in no case, and worse than other approaches in no case. It can be clearly seen that whether the evaluation index is HS or NMI, the statistical results of FREC are better than other methods in most cases, especially for the HS indicator, FREC can surpass all other algorithms on more than half of the datasets. Statistical analysis experiments show that in 100 repeated experiments, the overall performance of FREC is relatively stable, which is better than most algorithms.

4.6. Time complexity analysis

As shown in Algorithm 4, the computing cost of the proposed FREC mainly includes three parts: (1) For UDC, this function mainly consists of three loops with a time complexity of $O(mk(k-1))$. In particular, each instance needs to traverse to find the lower approximation when calculating UD in the inner loop, and this process will consume $O(n^2)$; (2) As for CMC, this part mainly calculates the upper triangular matrix of $\tilde{A}$, and the time complexity is $O(n^2k)$; (3) Finally, CSC computes the eigenvectors of adjacency matrix and performs fast clustering, with a time com-

Table 6
NMI results of FREC versus other ensemble algorithms

Dataset	*Heart*		*Cleveland*		*Dermatology*		*Movement*		*Appendicitis*	
Algorithm	Ave	Best	Ave	Best	Ave	Best	Ave	Best	Ave	Best
LWEA	0.192 v	0.192	0.221 v	0.221	0.875 v	0.875	0.581 v	0.581	0.041 v	0.041
LWGP	0.214 v	0.214	0.232 v	0.232	0.867 v	0.867	0.590 v	**0.611**	0.220 v	0.221
PTA	0.001 v	0.001	0.194 v	0.194	0.648 v	0.648	0.578 v	0.578	0.041 v	0.041
PTGP	0.001 v	0.001	0.197 v	0.197	0.648 v	0.648	0.581 v	0.589	0.041 v	0.041
ECPCSHC	0.001 v	0.001	0.217 v	0.217	0.912 v	0.912	0.564 v	0.564	0.185 v	0.185
ECPCSMC	0.242 v	0.242	0.224 v	0.224	0.912 v	0.912	0.593 v	0.594	0.157 v	0.157
WEAC	0.199 v	0.199	0.219 v	0.219	0.877 v	0.877	0.594 v	0.594	0.130 v	0.130
GPMGLA	0.234 v	0.234	0.229 v	0.229	0.906 v	0.906	0.597 v	0.597	0.157 v	0.157
SEC	0.231 v	**0.389**	0.216 v	**0.295**	0.758 v	0.923	0.547 v	0.606	0.127 v	**0.369**
DTCR	0.287 v	0.287	0.227 v	0.231	0.905 v	0.905	0.460 v	0.460	**0.294** *	0.294
RTFN	0.382 v	0.382	**0.245** *	0.245	0.869 v	0.923	0.584 v	0.584	0.241 v	0.241
FREC	**0.389**	**0.389**	0.234	0.234	**0.925**	**0.925**	**0.598**	0.598	0.247	0.247
Summary	(11/0/0)		(10/0/1)		(11/0/0)		(11/0/0)		(10/0/1)	

Dataset	*Led7digit*		*Mammographic*		*Cardio*		*IS*		*SPF*	
Algorithm	Ave	Best	Ave	Best	Ave	Best	Ave	Best	Ave	Best
LWEA	0.567 v	0.567	0.007 v	0.007	0.353 v	0.353	0.571 v	0.571	0.333 v	0.333
LWGP	0.573 v	0.577	0.007 v	0.007	0.357	0.369	0.584 v	0.617	0.326 v	0.349
PTA	0.486 v	0.486	0.007 v	0.007	0.318 v	0.318	**0.669** *	**0.669**	0.300 v	0.300
PTGP	0.497 v	0.524	0.007 v	0.007	0.316 v	0.343	0.618 v	0.650	0.294 v	0.336
ECPCSHC	0.487 v	0.487	0.007 v	0.007	0.355 v	0.355	0.566 v	0.566	0.305 v	0.305
ECPCSMC	0.559 v	0.560	0.002 v	0.002	0.353 v	0.356	0.562 v	0.562	0.314 v	0.314
WEAC	0.556 v	0.556	0.237 v	0.237	0.366 *	0.366	0.571 v	0.571	0.334 v	0.334
GPMGLA	0.572 v	0.572	0.002 v	0.002	**0.373** *	**0.373**	0.563 v	0.563	0.311 v	0.311
SEC	0.526 v	0.585	0.104 v	0.292	0.303 v	0.354	0.505 v	0.660	0.275 v	**0.363**
DTCR	0.480 v	0.480	**0.300** *	**0.300**	0.310 v	0.310	0.555 v	0.555	0.210 v	0.210
RTFN	0.584 v	0.585	0.292 v	0.292	0.361 *	0.361	0.575 v	0.575	0.339 v	0.339
FREC	**0.610**	**0.610**	0.295	0.295	0.358	0.359	0.643	0.643	**0.342**	0.361
Summary	(11/0/0)		(10/0/1)		(7/1/3)		(10/0/1)		(11/0/0)	

plexity of $O(ndk)$. Thus, the total cost of FREC is $O(mk(k-1)+n^2+ndk)$.

To compare the running time gap with other methods, the running time (seconds) of each algorithm is reported in Table 7. The experimental CPU used is i7-12700, and the memory is 24G. It can be seen that after considering the data features, the running time of FREC is significantly higher than that of other comparison methods. Especially as the number of instances continues to increase, the time of FREC increases significantly. In comparison, methods such as LWEA, SEC, and RTFN have achieved better running time. The above implementation shows that the time efficiency of FREC is relatively poor, which requires further optimisation in subsequent work.

5. Conclusion

This paper explores the role of considering cluster reliability using fuzzy-rough set in co-occurrence based ensemble clustering, and guides a fuzzy-rough ensemble approach. The experimental results indicate that the reliability induced by fuzzy-rough lower approximation is effective and can be reasonably employed in the task of ensemble clustering. Compared with other ensemble algorithms that ignore attributes and only employ base clustering results, FREC demonstrates the advantage of viewing feature information. Meanwhile, compared with the parallel version and base clustering, FREC shows its superiority again.

Nonetheless, from the time experiment, the efficiency of FREC is relatively slow. This is mainly due to the high time complexity of the algorithm. For large sample datasets, it will take a lot of time to calculate the lower approximation for each object. In future work, the idea of KD-tree [44] can be introduced to improve the running speed of the algorithm further. In addition, in Equation (23), if the two instances do not belong to the same cluster, it may not be a better choice to assign the adjacency matrix to 0 directly. Further mining the implicit connection

Table 7
Time complexity comparison of different algorithms (seconds)

Dataset	LWEA	LWGP	PTA	PTGP	ECPCSHC	ECPCSMC	WEAC	GPMGLA	SEC	DTCR	RTFN	FREC
Heart	0.01	0.12	0.02	0.06	0.18	0.21	0.01	1.65	0.01	36.36	1.34	18.76
Cleveland	0.01	0.18	0.02	0.05	0.22	0.25	0.01	2.54	0.01	38.52	1.47	19.50
Dermatology	0.01	0.11	0.01	0.06	0.24	0.31	0.01	3.47	0.01	227.09	1.49	19.59
Movement	0.01	0.11	0.02	0.06	0.20	0.23	0.01	2.43	0.01	437.69	1.63	22.41
Appendicitis	0.01	0.12	0.01	0.05	0.05	0.06	0.01	0.36	0.01	15.51	0.18	4.34
Led7digit	0.01	0.13	0.01	0.05	0.37	0.35	0.06	4.81	0.01	28.61	2.64	36.49
Mammographic	0.01	0.31	0.01	0.04	0.76	0.72	0.16	12.80	0.01	38.08	2.81	76.43
Cardio	0.01	0.54	0.01	0.10	3.37	2.57	1.45	55.96	0.01	368.16	4.52	404.51
IS	0.01	0.56	0.01	0.06	3.84	3.27	1.60	72.76	0.01	352.29	4.48	398.55
SPF	0.01	0.39	0.01	0.06	2.76	2.21	1.13	52.29	0.01	428.80	4.36	407.69

between instances of different clusters helps improve the clustering performance.

Whilst promising, further work remains. The performance of the ensemble strategy and multi-density cluster designs is worth further exploration. In addition, the implied relationship of the objects in the same base clustering but the different clusters is a valuable route of investigation. Moreover, a more comprehensive comparison of ensemble methods over diverse datasets from the real-world domains, such as mammographic risk assessment [46, 47] would construct the foundation for a broader series of issues for future research.

References

[1] A. Nazari, A. Dehghan, S. Nejatian, V. Rezaie and H. Parvin, A comprehensive study of clustering ensemble weighting based on cluster quality and diversity, *Pattern Analysis and Applications* **22** (2019), 133–145.

[2] A. Zubaroğlu and V. Atalay, Data stream clustering: a review, *Artificial Intelligence Review* **54** (2021), 1201–1236.

[3] A. Topchy, A.K. Jain and W. Punch, A mixture model for clustering ensembles, *Proceedings of the 2004 SIAM International Conference on Data Mining*, (2004), 379–390.

[4] A. Topchy, A.K. Jain and W. Punch, Clustering ensembles: Models of consensus and weak partitions, *IEEE Transactions on Pattern Analysis and Machine Intelligence* **27** (2005), 1866–1881.

[5] A.L. Fred and A.K. Jain, Combining multiple clusterings using evidence accumulation, *IEEE Transactions on Pattern Analysis and Machine Intelligence* **27** (2005), 835–850.

[6] A.M. Radzikowska and E.E. Kerre, A comparative study of fuzzy rough sets, *Fuzzy Sets and Systems* **126** (2002), 137–155.

[7] A. Karna and K. Gibert, Automatic identification of the number of clusters in hierarchical clustering, *Neural Computing and Applications* **34** (2022), 119–134.

[8] A. Ghosal, A. Nandy, A.K. Das, S. Goswami and M. Panday, A short review on different clustering techniques and their applications, *Emerging Technology in Modelling and Graphics*, (2020), 69–83.

[9] C. Li, M. Cerrada, D. Cabrera, R.V. Sanchez, F. Pacheco, G. Ulutagay and J. Valente de Oliveira, A comparison of fuzzy clustering algorithms for bearing fault diagnosis, *Journal of Intelligent & Fuzzy Systems* **34** (2018), 3565–3580.

[10] C.G. Arisdakessian, O.D. Nigro, G.F. Steward, G. Poisson and M. Belcaid, CoCoNet: an efficient deep learning tool for viral metagenome binning, *Bioinformatics* **37** (2021), 2803–2810.

[11] C. Wu, Q. Peng, J. Lee, K. Leibnitz and Y. Xia, Effective hierarchical clustering based on structural similarities in nearest neighbor graphs, *Knowledge-Based Systems* **228** (2021), 107295.

[12] D. Dubois and H. Prade, Putting rough sets and fuzzy sets together, *Intelligent Decision Support: Handbook of Applications and Advances of the Rough Sets Theory*, 1992.

[13] D. Li, H. Zhang, T. Li, A. Bouras, X. Yu and T. Wang, Hybrid missing value imputation algorithms using fuzzy c-means and vaguely quantified rough set, *IEEE Transactions on Fuzzy Systems* **30** (2021), 1396–1408.

[14] D. Huang, C.-D. Wang and J.-H. Lai, Locally weighted ensemble clustering, *IEEE Transactions on Cybernetics* **48** (2017), 1460–1473.

[15] D. Huang, J. Lai and C. Wang, Combining multiple clusterings via crowd agreement estimation and multi-granularity link analysis, *Neurocomputing* **170** (2015), 240–250.

[16] D. Huang, J. Lai and C. Wang, Robust ensemble clustering using probability trajectories, *IEEE Transactions on Knowledge and Data Engineering* **28** (2015), 1312–1326.

[17] D. Huang, J. Lai and C. Wang, Ensemble clustering using factor graph, *Pattern Recognition* **50** (2016), 131–142.

[18] D. Huang, C. Wang, H. Peng, J. Lai and C. Kwoh, Enhanced ensemble clustering via fast propagation of cluster-wise similarities, *IEEE Transactions on Systems, Man and Cybernetics: Systems* **51** (2018), 508–520.

[19] D. Huang, C. Wang, J. Wu, J. Lai and C. Kwoh, Ultra-scalable spectral clustering and ensemble clustering, *IEEE Transactions on Knowledge and Data Engineering* **32** (2019), 1212–1226.

[20] E. Rashedi and A. Mirzaei, A hierarchical clusterer ensemble method based on boosting theory, *Knowledge-Based Systems* **45** (2013), 83–93.

[21] F. Saeed, N. Salim and A. Abdo, Voting-based consensus clustering for combining multiple clusterings of chemical structures, *Journal of Cheminformatics* **4** (2012), 1–8.

[22] F. Yang, X. Li, Q. Li and T. Li, Exploring the diversity in cluster ensemble generation: Random sampling and random projection, *Expert Systems with Applications* **41** (2014), 4844–4866.

[23] G. Karypis and V. Kumar, A fast and high quality multilevel scheme for partitioning irregular graphs, *SIAM Journal on Scientific Computing* **20** (1998), 359–392.

[24] G. Li, M.R. Mahmoudi, S.N. Qasem, B.A. Tuan and K.-H. Pho, Cluster ensemble of valid small clusters, *Journal of Intelligent & Fuzzy Systems* **39** (2020), 525–542.
[25] H.Q. Liu, Q. Zhang and F. Zhao, Interval fuzzy spectral clustering ensemble algorithm for color image segmentation, *Journal of Intelligent & Fuzzy Systems* **35** (2018), 5467–5476.
[26] H. Liu, J. Wu, T. Liu, D. Tao and Y. Fu, Spectral ensemble clustering via weighted k-means: Theoretical and practical evidence, *IEEE Transactions on Knowledge and Data Engineering* **29** (2017), 1129–1143.
[27] H. Xing, Z. Xiao, R. Qu, Z. Zhu and B. Zhao,An efficient federated distillation learning system for multitask time series classification, *IEEE Transactions on Instrumentation and Measurement* **71** (2022), 1–12.
[28] H. Xing, Z. Xiao, D. Zhan, S. Luo, P. Dai and K. Li, SelfMatch: Robust semisupervised time-series classification with self-distillation, *International Journal of Intelligent Systems* **37** (2022), 8583–8610.
[29] J. Yi, T. Yang, R. Jin, A.K. Jain and M. Mahdavi, Robust ensemble clustering by matrix completion, *2012 IEEE 12th International Conference on Data Mining*, (2012), 1176–1181.
[30] J. Zhu, J. Jang-Jaccard, T. Liu and J. Zhou, Joint spectral clustering based on optimal graph and feature selection, *Neural Processing Letters* **53** (2021), 257–273.
[31] J.C. Fodor, Contrapositive symmetry of fuzzy implications, *Fuzzy Sets and Systems* **69** (1995), 141–156.
[32] K. Golalipour, E. Akbari, S.S. Hamidi, M. Lee and R. Enayatifar, From clustering to clustering ensemble selection: A review, *Engineering Applications of Artificial Intelligence* **104** (2021), 104388.
[33] L. Franek and X. Jiang, Ensemble clustering by means of clustering embedding in vector spaces, *Pattern Recognition* **47** (2014), 833–842.
[34] MacQueen, Some methods for classification and analysis of multivariate observations. *Proceedings of the Fifth Berkeley Symposium on Mathematical Statistics and Probability* **1** (1967), 281–297.
[35] M. Zhang, Weighted clustering ensemble: A review, *Pattern Recognition*, (2021), 108428.
[36] N. Iam-On, T. Boongoen and S. Garrett, Lce: a link-based cluster ensemble method for improved gene expression data analysis, *Bioinformatics* **26** (2010), 1513–1519.
[37] Q. Ma, J. Zheng, S. Li and G. Cottrell, Learning representations for time series clustering, *Advances in Neural Information Processing Systems* **32** (2019).
[38] R. Jensen and Q. Shen, New approaches to fuzzy-rough feature selection, *IEEE Transactions on Fuzzy Systems* **17** (2008), 824–838.
[39] S. Khedairia and M.T. Khadir, A multiple clustering combination approach based on iterative voting process, *Journal of King Saud University-Computer and Information Sciences* **34** (2022), 1370–1380.
[40] T. Li and C. Ding, Weighted consensus clustering, *Proceedings of the 2008 SIAM International Conference on Data Mining*, (2008), 798–809.
[41] T. Zhang, F. Ma, D. Yue, C. Peng and G.M. O'Hare, Interval type-2 fuzzy local enhancement based rough k-means clustering considering imbalanced clusters, *IEEE Transactions on Fuzzy Systems* **28** (2019), 1925–1939.
[42] U. Von Luxburg, A tutorial on spectral clustering, *Statistics and Computing* **17** (2007), 395–416.
[43] X. Peng, H. Zhu, J. Feng, C. Shen, H. Zhang and J.T. Zhou, Deep clustering with sample-assignment invariance prior, *IEEE Transactions on Neural Networks and Learning Systems* **31** (2019), 4857–4868.
[44] Y. Chen, L. Zhou, N. Bouguila, C. Wang, Y. Chen and J. Du, Block-dbscan: Fast clustering for large scale data, *Pattern Recognition* **109** (2021), 107624.
[45] Y. Li, J. Yu, P. Hao and Z. Li, Clustering ensembles based on normalized edges, *Pacific-Asia Conference on Knowledge Discovery and Data Mining*, (2007), 664–671.
[46] Y. Qu, G. Yue, C. Shang, L. Yang, R. Zwiggelaar and Q. Shen, Multi-criterion mammographic risk analysis supported with multi-label fuzzy-rough feature selection, *Artificial Intelligence in Medicine* **100** (2019), 101722.
[47] Y. Qu, Q. Fu, C. Shang, A. Deng, R. Zwiggelaar, M. George and Q. Shen, Fuzzy-rough assisted refinement of image processing procedure for mammographic risk assessment, *Applied Soft Computing* **91** (2020), 106230.
[48] Y. Yao, Relational interpretations of neighborhood operators and rough set approximation operators, *Information Sciences* **111** (1998), 239–259.
[49] Z. Pawlak, Rough sets: Theoretical aspects of reasoning about data, *Springer Science & Business Media* **9** (2012).
[50] Z. Xiao, X. Xu, H. Xing, S. Luo, P. Dai and D. Zhan, RTFN: a robust temporal feature network for time series classification, *Information Sciences* **571** (2021), 65–86.